Title

Endoglin Is Essential for the Maintenance of Self-Renewal and Chemoresistance in Renal Cancer Stem Cells.

Journal

Stem cell reports, 9(2)

ISSN

2213-6711

Authors

Hu, Junhui
Guan, Wei
Liu, Peijun
et al.

Publication Date

2017-08-01

DOI

10.1016/j.stemcr.2017.07.009

Peer reviewed

Stem Cell Reports
Article

ISSCR

OPEN ACCESS

Endoglin Is Essential for the Maintenance of Self-Renewal and Chemoresistance in Renal Cancer Stem Cells

Junhui Hu,[1,2,4,7] Wei Guan,[1,7] Peijun Liu,[1] Jin Dai,[3] Kun Tang,[1] Haibing Xiao,[1] Yuan Qian,[6] Allison C. Sharrow,[4] Zhangqun Ye,[1] Lily Wu,[4,5,*] and Hua Xu[1,*]

[1]Department of Urology and Institute of Urology, Tongji Hospital, Tongji Medical College, Huazhong University of Science and Technology (HUST), Wuhan 430030, China
[2]Department of Pediatric Surgery, Tongji Hospital, Tongji Medical College, Huazhong University of Science and Technology (HUST), Wuhan 430030, China
[3]Department of Urology, The First Affiliated Hospital of Yangtze University, Jingzhou 434000, China
[4]Department of Molecular and Medical Pharmacology, David Geffen School of Medicine, University of California at Los Angeles, Los Angeles, CA 90095, USA
[5]Department of Urology, David Geffen School of Medicine, University of California at Los Angeles, Los Angeles, CA 90095, USA
[6]MoE Key Laboratory for Biomedical Photonics, Department of Biomedical Engineering, Huazhong University of Science and Technology, Wuhan 430074, China
[7]Co-first author
*Correspondence: lwu@mednet.ucla.edu (L.W.), xuhua@mail.hust.edu.cn (H.X.)
http://dx.doi.org/10.1016/j.stemcr.2017.07.009

SUMMARY

Renal cell carcinoma (RCC) is a deadly malignancy due to its tendency to metastasize and resistance to chemotherapy. Stem-like tumor cells often confer these aggressive behaviors. We discovered an endoglin (CD105)-expressing subpopulation in human RCC xenografts and patient samples with a greater capability to form spheres *in vitro* and tumors in mice at low dilutions than parental cells. Knockdown of CD105 by short hairpin RNA and CRISPR/cas9 reduced stemness markers and sphere-formation ability while accelerating senescence *in vitro*. Importantly, downregulation of CD105 significantly decreased the tumorigenicity and gemcitabine resistance. This loss of stem-like properties can be rescued by *CDA*, *MYC*, or *NANOG*, and *CDA* might act as a demethylase maintaining *MYC* and *NANOG*. In this study, we showed that Endoglin (CD105) expression not only demarcates a cancer stem cell subpopulation but also confers self-renewal ability and contributes to chemoresistance in RCC.

INTRODUCTION

Renal cell carcinoma (RCC) accounts for almost 3% of all malignancies worldwide, ranking the seventh most common cancer in men and the ninth in women. Every year approximately 209,000 newly diagnosed cases and 102,000 deaths can be attributed to this disease across the world (Siegel et al., 2013). RCC is a highly metastatic malignancy, as 30% of the patients present with metastatic disease at diagnosis and one-third of the patients with localized disease will relapse with distant metastasis after nephrectomy (Hoffman and Cairns, 2011; Linehan and Rathmell, 2012; Sudarshan et al., 2013). Several oncogenes have been identified to be involved in the pathogenesis of RCC, such as *VHL* in clear cell RCC (ccRCC) and *MET* in hereditary papillary RCC (Pantuck et al., 2010; Rini et al., 2009). Treatments that target the downstream effectors of these oncogenic steps, such as blocking the *VEGF* axis with the antibody bevacizumab (Escudier et al., 2008) or kinase inhibitor sorafenib (Larkin and Eisen, 2006), have slightly improved progression-free survival. However, there is a lack of treatment for relapsed or metastatic RCC. Consequently, the outcome of this group of patients is very poor, with 5-year survival of only 11% (Larkin and Eisen, 2006).

A large volume of evidence supports the existence of cancer stem cells (CSCs), a rare subpopulation within solid tumors that are resistant to therapy. Furthermore, their high capacity for self-renewal enables CSCs to support tumor relapse after treatment (Chiou et al., 2010; Lee et al., 2011). One of the major challenges in the field is to identify rare CSCs in solid tumors. Specifically, not a single universal marker is capable of identifying a CSC. It is likely that distinctive markers are needed to isolate CSCs from different tumor types. Bussolati et al. (2008) reported CD105 (endoglin) as a CSC marker in human kidney cancer. They showed that as few as 100 $CD105^+$ cells can form tumors in NOD/SCID mice. However, no follow-up study has investigated the therapeutic potential of targeting this $CD105^+$ population except the differentiation therapy by interleukin-15 (Azzi et al., 2011). In this study, we further investigated the $CD105^+$ population in human RCC xenograft models and found that CD105 is not only a biomarker for renal CSCs but can also serve as a functional target for therapeutic intervention.

RESULTS

Xenograft Tumor-Derived $CD105^+$ Subpopulation Displays Stem-like Characteristics with Slow Proliferation and Increased Self-Renewal

To gain a better understanding of the contribution of CD105 to stem-like cells in human kidney cancer, we analyzed its expression in several kidney cancer cell lines, including

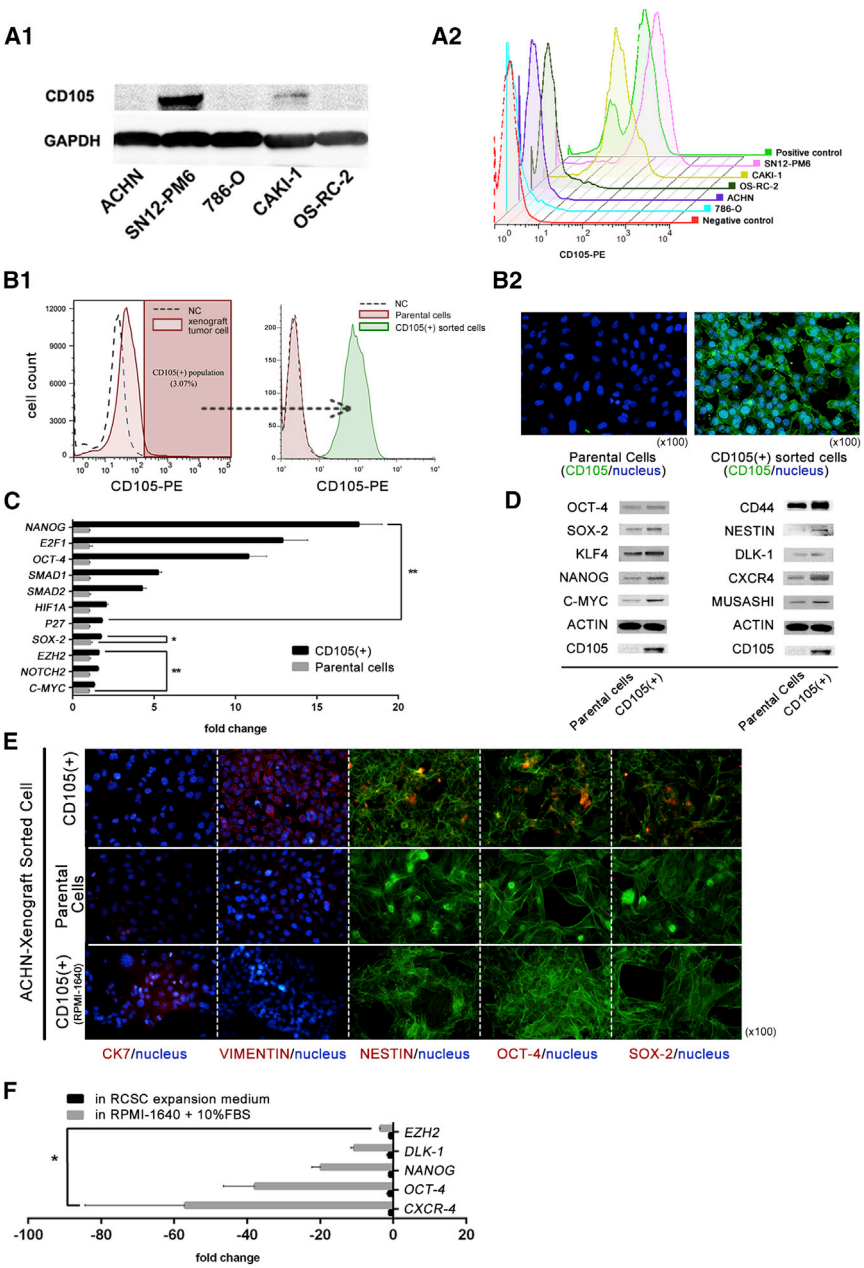

Figure 1. Xenograft Tumor-Derived CD105$^+$ Subpopulation Displays Stem-like Characteristics with Potential to Differentiate

(A) The relative CD105 expression profile of different human kidney cancer cell lines (786-O, ACHN, OS-RC-2, CAKI-1, and SN12-PM6) is shown in western blotting (A1) and flow cytometry (in which the positive control is human histiocytic lymphoma cell line U-937) (A2).

(B) After cell sorting, ACHN-CD105$^+$ cells showed remarkably high expression (100%) of CD105 according to both flow cytometry (B1) and immunofluorescence staining (B2). (C–F) qRT-PCR (C), western blotting (D), and immunofluorescence staining (E) were used to assess the stemness-related gene expression in the sorted ACHN-CD105$^+$ cells and its parental cell line. Also, as we cultured the sorted CD105$^+$ cells in nutrient-enriched differentiation medium RPMI-1640 + 10% FBS for 2 weeks, immunofluorescence (E) and qRT-PCR (F) were used to analyze the changes in epithelial marker CK7, mesenchymal marker VIMENTIN, and stemness markers such as NESTIN and OCT-4 (three independent experiments were undertaken for each assay. All error bars indicate the mean ± SD. *$p < 0.05$; **$p < 0.01$).

786-O, ACHN, OS-RC-2, CAKI-1, and SN12-PM6. Comparative analysis of CD105 expression in the whole cell population at the protein (Figure 1A1 and 1A2) level revealed the highest level of expression in SN12-PM6 and lowest in 786-O. SN12PM6 is a highly metastatic derivative of SN12C kidney cancer cell line developed by Fidler and coworkers in 1989 (Naito et al., 1989). CAKI-1 is a metastatic kidney cancer cell line derived from skin metastasis according to the American Type Culture Collection. If CD105 defines a CSC population, then only a small fraction of the whole tumor cell population is expected to express this marker. Indeed, the fraction of CD105$^+$ cells ranges from 0.03% (786-0) to 0.06% (ACHN) to 2.17% (OS-RC2). The SN12PM6 cell line and CAKI-1 are the two exception cell lines with 93.9% and 90.93% cells expressing CD105, respectively (Figure 1A2). Scientists have expressed concern as to the relevance of CSCs isolated from tumor cell lines cultured long-term *in vitro* compared with those from *in vivo* sources. Thus, we modified our methods to analyze the CD105$^+$ populations from human kidney cancer xenograft established in NOD/SCID mice (Figure S1A). We took great caution to ensure the CD105$^+$ cells thus harvested were

indeed of human origin with little murine cell contamination by using PCR to assess the level of human- and mouse-specific cytochrome C oxidase I gene (Parodi et al., 2002) (Table S1 and Figure S1B). We analyzed the CD105$^+$ population in xenografts derived from the canonical human kidney cancer cell line, ACHN. As illustrated in Figure 1B1, the CD105$^+$ cells form a distinct population that represents 3% of the total cells within the tumor. The expression of CD105 in each cell is remarkably robust (Figure 1B2).

A large set of stemness genes is often upregulated in CSCs (Beier et al., 2007; Chiou et al., 2010; Kumar et al., 2012). We verified that *NANOG*, *OCT-4*, *SOX-2*, *KLF-4*, *C-MYC* (Beier et al., 2007; Chiou et al., 2010; Kumar et al., 2012), *SMAD1* (Kandyba et al., 2014), *SMAD2* (Sakaki-Yumoto et al., 2013), *HIF1A* (Li et al., 2014), *DLK-1* (Whalley, 2011), and *EZH2* (Kim et al., 2015) are significantly upregulated in the ACHN CD105$^+$ compared with the parental population by qRT-PCR (Figure 1C) and western blot (Figure 1D). The heightened expression of stemness markers in the CD105$^+$ population was further verified by immunofluorescent cellular staining, and representative images of NESTIN, OCT-4, and SOX-2 stains are shown in Figure 1E. Likewise, these stemness genes are also upregulated in the CD105$^+$ population in OS-RC-2 and 786-O tumors (Figure S1D1 and S1D2). Thus far, these results demonstrate the feasibility of isolating CD105$^+$ cells from human kidney cancer xenografts to study the biology of renal CSCs.

Next, we examined the stem-like properties of the CD105$^+$ population. We examined the differentiation potential of the CD105$^+$ cells by culturing in differentiation medium in either RPMI-1640 plus 10% fetal bovine serum (FBS) or DMEM high-glucose (DMEM-HG) plus 10% FBS. The starting CD105$^+$ population appeared to be mesenchymal-like with high expression of VIMENTIN and low expression of cytokeratin 7 (CK7) (Figure 1E, left panel). After culturing for 2 weeks in RPMI-1640 with 10% FBS, the population converted to epithelial-like cells with increased expression of CK7 and decreased VIMENTIN (Figure 1E). The cellular differentiation occurred concurrently with the downregulation of a set of stemness-related genes including *CXCR4*, *OCT-4*, *NANOG*, *DLK-1*, and *EZH2* (Figure 1F). Similar results were also observed with DMEM-HG with 10% FBS (Figure S1C). We next analyzed the growth characteristics of this CSC population. Cell-cycle analysis showed that a much higher proportion (13.48% ± 2.74%) of CD105$^+$ were arrested in G_0 stage than in the parental population (2.84% ± 0.59%) (Figure 2A), which is also seen in hepatocellular CSCs (Kamohara et al., 2008). Consistent with the idea that the CSC population is a dormant one, we also found that CD105$^+$ cells proliferated more slowly than the parental population as measured by the colorimetric cell-counting CCK8 assay (Figure 2B), 5-ethynyl-2′-deoxyuridine (EdU) assay to measure DNA synthesis (Figure 2C), and colony-formation assay (Figure 2D). Furthermore, the proportion of cell population undergoing senescence, identified by a positive β-galactosidase staining, was much higher in parental population than in CD105$^+$ cells, which indicated that the CD105$^+$ population is "younger" (Figure 2E). In the sphere-formation assay, the CD105$^+$ cells produced 3-fold more spheres than the parental population, indicating its higher self-renewal potential (Figure 2F).

CD105 Demarcates a Chemotherapy-Resistant Population

CSCs are thought to be the subpopulation that can withstand and survive therapeutic insults, eventually leading to disease relapse and progression. To investigate chemotherapy resistance in our model, we analyzed the response of CD105$^+$ and parental populations to two common chemotherapeutic agents, cisplatin and gemcitabine. As shown in Figure 3A, CD105$^+$ cells were found to be more resistant to cisplatin with a maximum inhibitory concentration (IC_{50}) of 107.15 ± 1.33 μM compared with an IC_{50} of 49.96 ± 1.05 μM for the parental population after 72 hr of treatment *in vitro*. The differential treatment response to gemcitabine showed a similar difference, with the estimated IC_{50} of 66.01 μM and 34.85 μM for the CD105$^+$ and parental populations, respectively (Figure 3B).

Next, we profiled the expression of several genes known to contribute to drug resistance in our models. As shown in Figure 3C, cytidine deaminase (*CDA*), activation-induced *CDA* (*AICDA*), and ATP-binding cassette (*ABC*) transporters such as *ABCB1*, *ABCC1*, *ABCC2*, and *ATM* are all upregulated in the CD105$^+$ population. *CDA* is dramatically upregulated by more than 1,000-fold, while *AICDA* is increased by more than 30-fold in the CD105$^+$ population (Figure 3C). *CDA* and *AICDA* are two important genes known to regulate resistance to gemcitabine by deaminating gemcitabine to 2′,2′-difluorodeoxyuridine.

ABC transporters are a class of membrane proteins that mediate chemoresistance by actively pumping chemotherapeutic agents out of the cells. In our analysis, *ABCC1*, *ABCC2*, *ABCB1*, and *ATMs* were found to be increased to different extents in the sorted CD105$^+$ population. Also, *SIRT1* (Chen et al., 2014), *SMAD1*/*SMAD2* (Paldino et al., 2014), *BCL2* (Ma et al., 2008), and *ATR* (Abdullah and Chow, 2013; Maugeri-Saccà et al., 2012), together with *ALDH1A3* (Canino et al., 2015) and *MGMT* (Beier et al., 2011), were all found to be upregulated (data not shown), which have also been reported in other CSCs or stem cells.

CD105$^+$ Cells Are More Tumorigenic than Parental Cells

Serial transplantation assay is one of the essential experiments to examine the tumor-initiating capabilities of

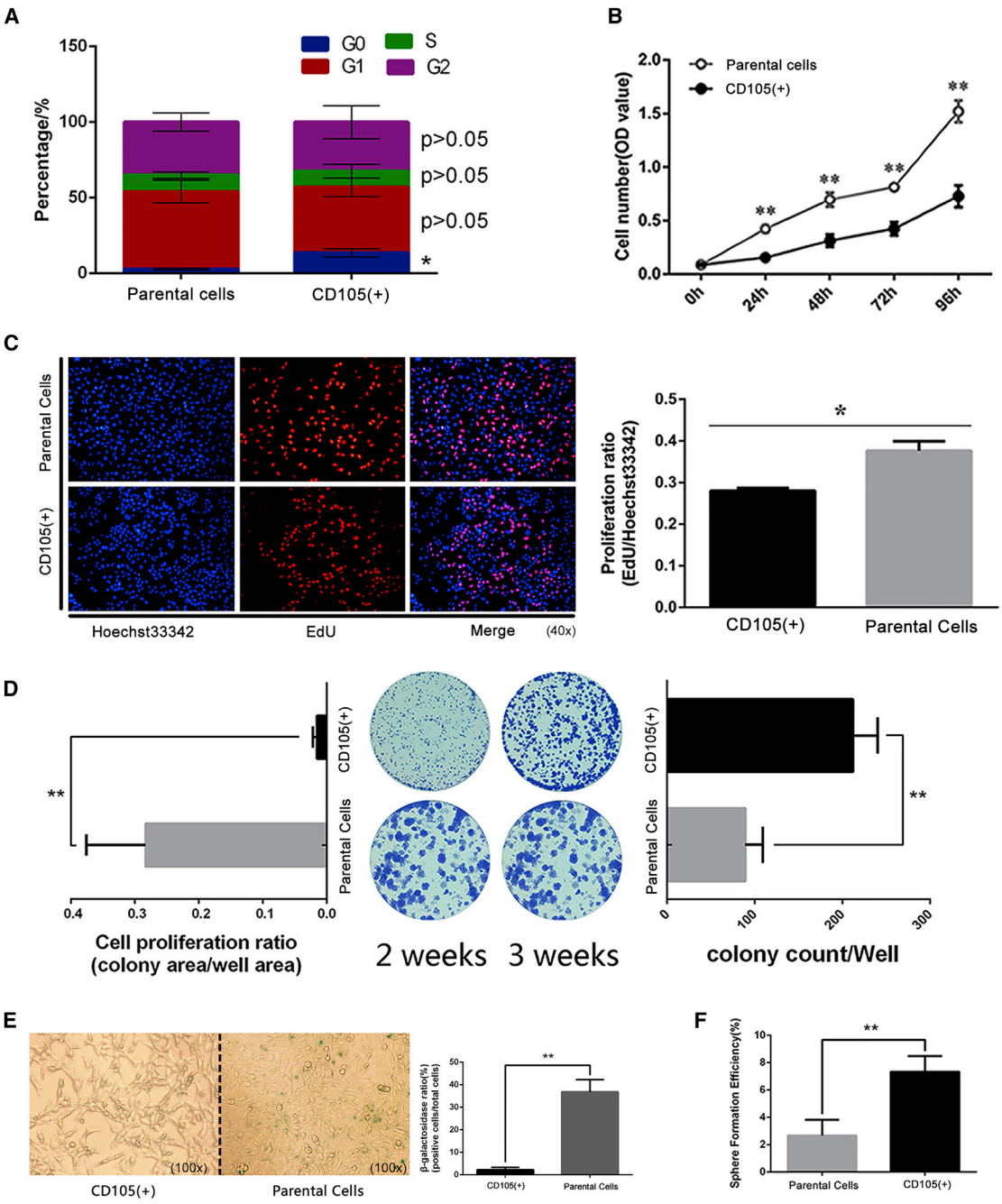

Figure 2. Xenograft Tumor-Derived CD105$^+$ Cells Are Less Proliferative with Increased Self-Renewal

(A) Cell-cycle analysis showed that a much higher proportion of CD105$^+$ cells were arrested in the G_0 stage (13.48% ± 2.74%) compared with the parental population (2.84% ± 0.59%).

(B–F) Colorimetric cell count CCK8 assay (B), EdU assay (C), and colony-formation assay (D) showed that CD105$^+$ cells proliferate more slowly than parental cells. However, the colony-formation assay (D), β-galactosidase assay (E), and sphere-formation assay (F) proved that CD105$^+$ subpopulation has an enhanced self-renewal capability is younger compared with parental cells.

Three independent experiments were undertaken for each assay. All error bars indicate the mean ± SD. *p < 0.05; **p < 0.01.

CSCs. As shown in Figure 4A, 1 × 10^2, 1 × 10^4, and 1 × 10^6 cells of CD105$^+$ and its parental cell line were injected into the subcapsular space of kidney in NOD/SCID mice. The CD105$^+$ group can produce tumors with as few as 1 × 10^2 cells. The heightened tumorigenicity of the CD105$^+$ population compared with the parental cell group was

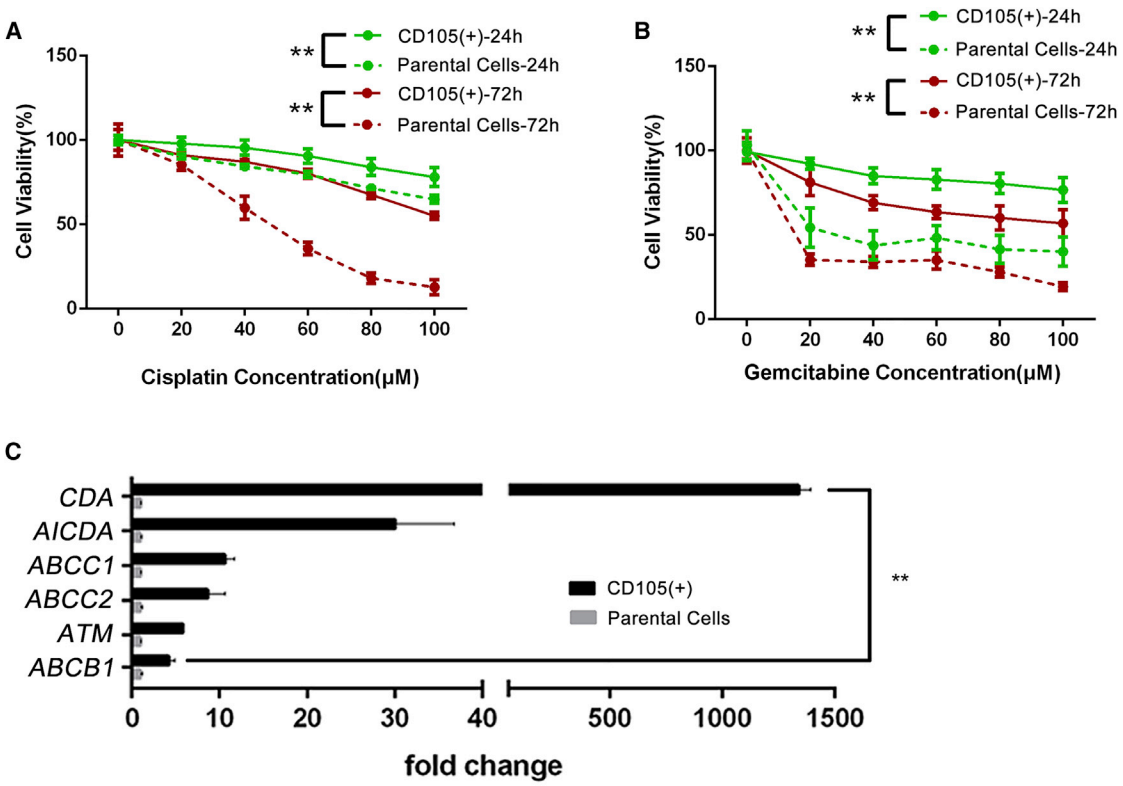

Figure 3. The CD105$^+$ Renal Cancer Subpopulation Is Resistant to Cisplatin and Gemcitabine with Elevated Chemoresistance Molecular Profile

(A and B) Chemoresistance assays with two classical chemotherapy agents for cancers: cisplatin (A) and gemcitabine (B).

(C) Chemoresistance-related gene profile analysis via qRT-PCR.

Three independent experiments were undertaken for each assay. All error bars indicate the mean ± SD. **p < 0.01.

demonstrated by the incidence and weight of tumor (Figures 4A and 4C). Additionally, labeling of cells with EGFP permitted *in vivo* fluorescence imaging (Figure 4B). To examine the tissue architecture of our tumor xenografts in finer detail, we employed immunohistochemical staining with human-specific MHC-I, which revealed a clear demarcation of the cancerous tissue from the adjacent normal renal glomeruli and distal tubules (Figure 4D).

Knockdown of CD105 Diminishes Self-Renewal Potential, which Can Be Rescued by *CDA*, *MYC*, or *NANOG*

To investigate the functionality of CD105, we employed short hairpin RNA (shRNA)-mediated knockdown technology and confirmed its effectiveness in downregulating CD105 expression by qRT-PCR (Figure 5A1) and western blotting (Figure 5A2). Interestingly, stemness genes *CXCR-4*, *NANOG*, *DLK1*, *SOX-2*, *OCT-4*, *KLF4*, and *C-MYC* were decreased concomitantly upon silencing of CD105 (Figure 5A3). CD105 knockdown also disables the self-renewal capability of CD105$^+$ cells as assessed by the sphere-formation assay, shown in Figure 5B1 and 5B2. Next we assessed whether forced re-expression of some of the downregulated genes after CD105 knockdown could restore self-renewal potential. Remarkably, overexpression of *CDA*, *MYC*, or *NANOG* individually in the CD105-silenced CD105$^+$ cells (CD105$^+$-shENG) was able to restore the sphere-forming capability (Figure 5C1 and 5C2), with concomitant upregulation of the stemness genes *CD105* (*ENG*), *CDA*, *MYC*, *NANOG*, *MEST*, *AICDA*, *CXCR4*, and *DLK-1*, but not *OCT-4*, as shown in Figures 5D–5F. The mechanism regulating the expression of these stemness genes are unknown at this time.

Knockdown of CD105 Debilitates Tumorigenicity, Accelerates Cell Senescence, and Abrogates Chemoresistance

Next we assessed the contribution of CD105 to tumor formation *in vivo*. As shown in Figure 6A1–6A3, renal tumor formation can be established by implanting as few as 1 × 10^2 CD105$^+$ cells. However, a much higher cell dosage was required to establish tumors with the CD105

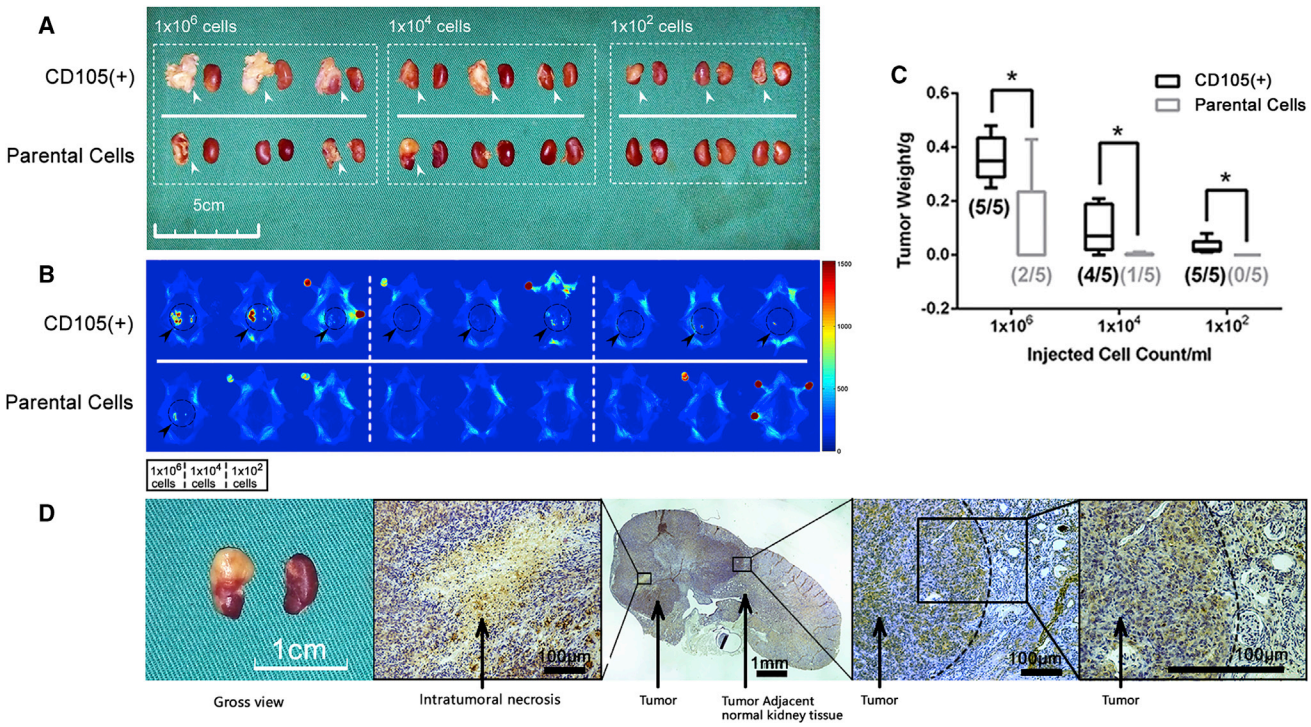

Figure 4. The CD105$^+$ Renal Cancer Subpopulation Is More Tumorigenic than CD105$^-$ Parental Cells *In Vivo*

(A and B) The *in vivo* orthotopic xenograft model shows that sorted CD105$^+$ cells are more capable of forming tumors in the kidney than its parental cells both in the gross view (A, arrowheads indicate the kidney with tumor) and in the *in vivo* imaging by GFP (B, circles pointed out by arrowheads indicate where kidney tumor developed).

(C) The tumor weight and the incidence of tumorigenesis between the two groups in (A) and (B).

(D) Representative figure showing the typical orthotopic kidney cancer in NOD/SCID mice and immunohistochemical staining with human-specific MHC-I antibody differentiating the tumor tissue and normal tissue.

Fifteen mice were used for each group and five for each cell dilution in each group, but only three in each cell dilution of each group are shown as representative. There were 30 mice in total for these two groups. All error bars indicate the mean ± SD. *$p < 0.05$.

knockdown cells (1 × 10^6/mouse). An increase in cell senescence brought on by CD105 silencing likely contributed to the reduced tumor-formation ability of these CD105$^+$-shENG cells (Figures 6B and S4A).

CSCs are postulated to play an integral role in chemotherapy resistance. Thus, we compared the impact of CD105 knockdown on gemcitabine sensitivity in CD105$^+$ cells. As shown in Figure 7A, silencing CD105 increased the sensitivity of these cells to gemcitabine, which was correlated with the downregulation of a set of chemoresistance genes (*ABCB1*, *ABCC1*, *ABCC2*, and *ATM*) together with deaminases (*CDA* and *AICDA*) (Figure 7B). Similar to the results observed for self-renewal and tumorigenicity, the forced overexpression of *CDA*, *MYC*, or *NANOG* in the CD105$^+$-shENG cells restored chemoresistance (Figures 7C–7E). To verify the chemoresistance of CD105$^+$ cells *in vivo*, ACHN tumors were established and treated with gemcitabine via intraperitoneal injection. The proportion of CD105$^+$ cells was found to be remarkably increased after gemcitabine treatment (Figure 7F), indicating that CD105$^+$ stem-like cells are the chemoresistant cell population *in vivo*. This finding has been corroborated by studies in lung cancer, ovarian cancer, colorectal cancer, and breast cancer.

DISCUSSION

The concept of "renal CSC" was investigated by Camussi and coworkers in 2003, when they isolated renal CSCs by fluorescence-activated cell sorting from ccRCC patients' tumor samples. Subsequently, Qiu and colleagues identified a cancer stem-like cell side population in the cell line 769P (Huang et al., 2013), and Zhong et al. (2010) adopted the sphere-formation assay to enrich CSCs within the human cancer cell line SK-RC-42. Similar CSC subpopulations have been widely reported in cell lines from other cancers, such as glioblastoma, prostate cancer, and gastric cancer. However, it remains controversial whether the cancer stem-like cells isolated from cell lines are equivalent to

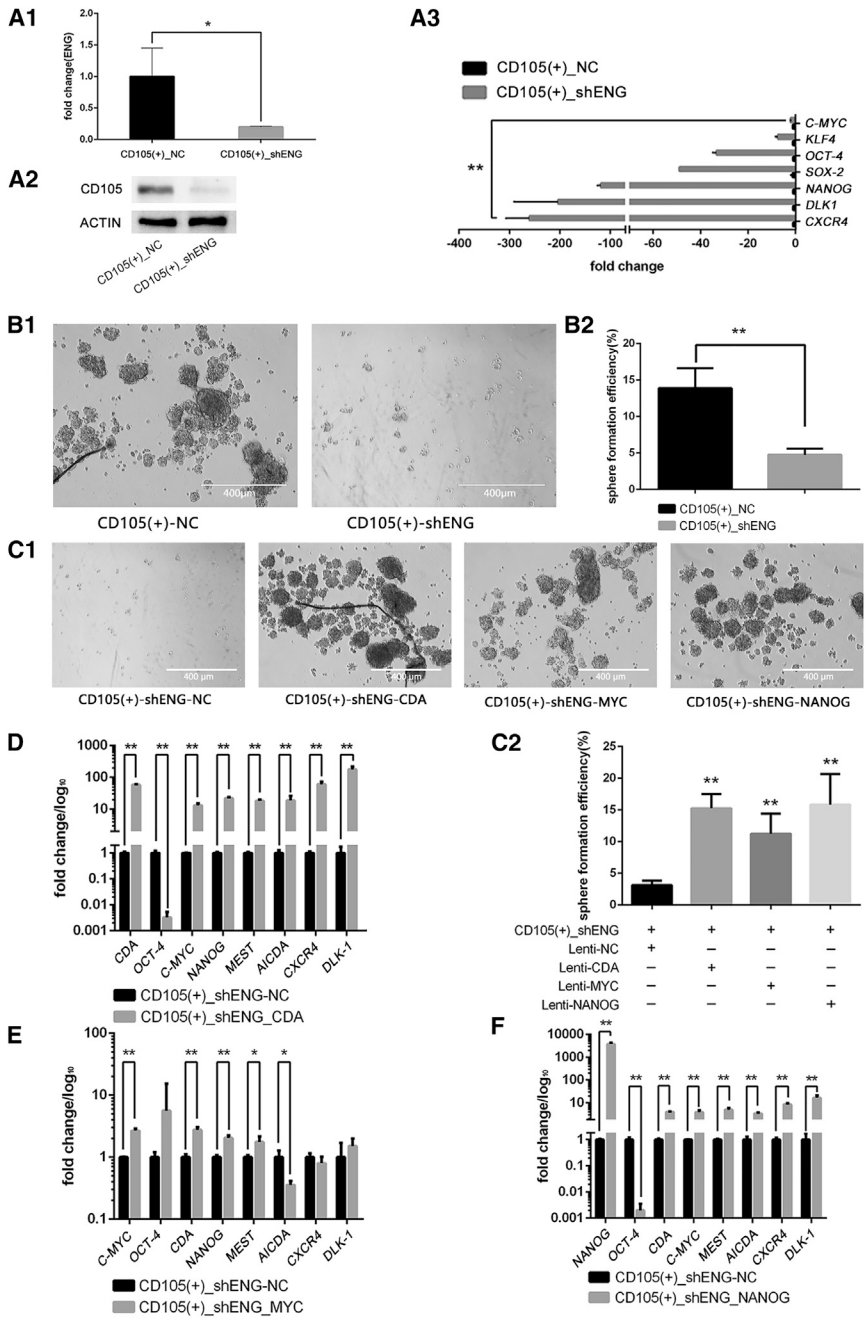

Figure 5. Knockdown of CD105 in the CD105$^+$ Renal Cancer Subpopulation Greatly Diminishes the Expression of Stemness Genes and Sphere-Formation Ability of *CDA*, *MYC*, and *NANOG*

(A)The knockdown of CD105 in ACHN-CD105$^+$ cell line was verified by qRT-PCR (A1) and western blotting (A2). Accompanied by CD105 downregulation, a series of stemness-related genes were found to be downregulated (A3), including NANOG, C-MYC, and CDA (see Figure 7B).

(B–F) Simultaneously, sphere-formation ability was also diminished after knockdown of CD105 in ACHN-CD105$^+$ cells (B1 and B2). After overexpressing NANOG, C-MYC, and CDA independently, the sphere-formation ability was rescued (C1 and C2) and the possible downstream gene expression profile were examined by qRT-PCR (D–F).

Three independent experiments were undertaken for each assay. *p < 0.05; **p < 0.01.

those isolated from *in vivo* sources. Many investigators incorporated additional functional phenotype-based methods such as sphere-formation assay, Hoechst dye-exclusion method, or aldehyde dehydrogenase (ALDH) activity assay to define the CSC population with more certainty. Although Khan et al. (2016) sorted CD105$^+$ populations from kidney cancer cell lines such as ACHN and CAKi-2, they failed to verify the CSC behavior of the sorted cell population *in vivo* and neglected the involvement of the tumor microenvironment in CSC development and maintenance (Borovski et al., 2011). Therefore, in this study we investigated the use of endoglin (CD105) to isolate putative renal CSCs from xenograft tumors derived from human kidney cancer cell lines rather than the cell lines, and explored CD105 function in renal CSCs. Interestingly, no statistical difference was found between the ACHN xenograft parental cells and the CD105$^+$ cells sorted directly from ACHN cell line in the sphere-formation assay

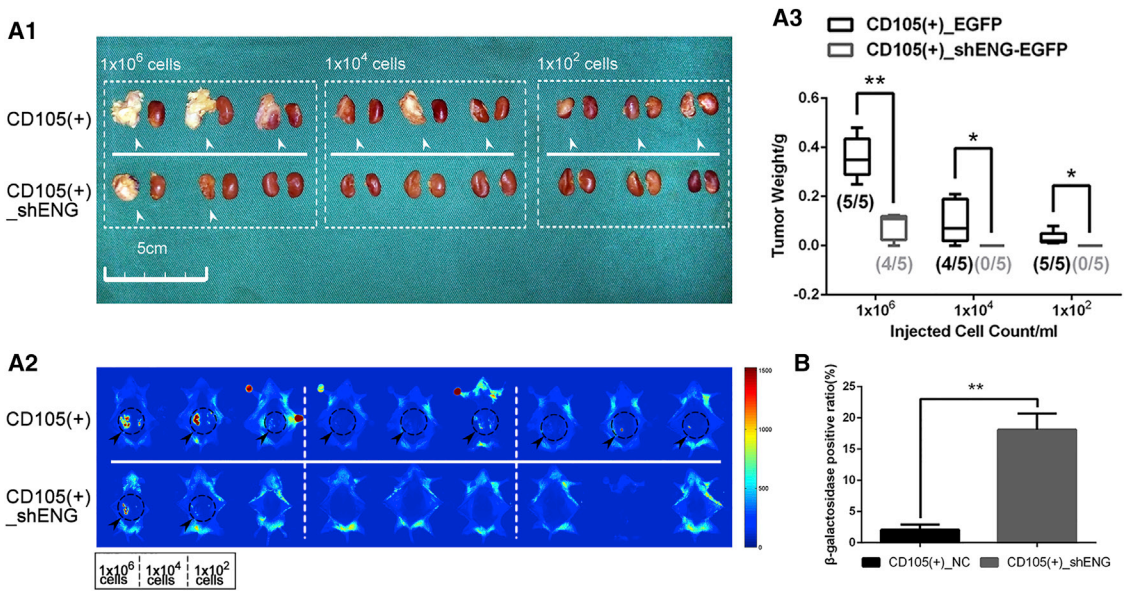

Figure 6. Knockdown of CD105 in CD105$^+$ Cells Debilitates the Tumorigenic Ability *In Vivo* and Accelerates Tumor Cell Senescence

(A) After knockdown of CD105 in ACHN-CD105$^+$ cells, *in vivo* orthotopic xenograft assay showed that the tumorigenicity of ACHN-CD105$^+$ cells was greatly diminished after CD105$^+$ knockdown both grossly (A1) and using *in vivo* imaging of EGFP (A2). Tumor incidence for each group as well as the tumor weight is shown in (A3).

(B) Cell senescence as measured by β-galactosidase, showing elevated senescence in the CD105 knockdown cells.

For the animal study, 15 mice were used for each group and five for each cell dilution in each group, but only three mice in each cell dilution of each group are shown as representative. There were 30 mice in total for these two groups. Three independent experiments were undertaken for cell senescence assay. *$p < 0.05$; **$p < 0.01$.

(Figure S2), indicating the difference of CD105$^+$ subpopulation from the cell line and the *in vivo* xenograft in their self-renewal potential, as well as the potential involvement of the tumor microenvironment. This modified methodology enabled us to identify a rare, but distinct, CD105-expressing population from several human kidney cancer xenografts that possess a prominent stemness gene signature, expressing high levels of *NANOG*, *C-MYC*, *KLF-4*, *OCT-4*, and *C-MYC*.

To functionally characterize the stemness of the CD105$^+$ population, we focused on xenografted ACHN tumors. The CD105$^+$ cells retain differentiation potential, and exhibit enhanced self-renewal, less senescence, and greater tumorigenicity compared with the parental population. Furthermore, the CSC population showed greatly increased expression of CDA, contributing to its chemoresistant phenotype. The CD105$^+$ cells are more quiescent with a higher proportion in the G_0 stage, a characteristic manifested in other CSC populations, such as the extreme case of melanoma JARID1B$^+$ cells, whose doubling time is over 4 weeks (Roesch et al., 2010). Interestingly, HIF1A is one of the critical factors involved in kidney cancer development and is known to suppress tumor cell growth (Shen et al., 2011). The upregulation of HIF1A in CD105$^+$ cells could in part contribute to the slow proliferation phenotype of this population (Schokrpur et al., 2016).

Endoglin (ENG, CD105) is a homodimer coreceptor in the transforming growth factor β (TGFβ) signaling pathway and primarily interacts with TGFβR-I and TGFβR-II, which serve as receptors primarily for TGFβI and TGFβIII, and to a lesser extent TGFβII (Guerrero-Esteo et al., 2002; Koleva et al., 2006). It is highly expressed in proliferating endothelial cells and immune cells. CD105 has been found to play a critical role in angiogenesis, as congenital mutation of CD105 leads to hereditary hemorrhagic telangiectasia type I, a syndrome of arteriovenous malformation and telangiectasia. Hence, earlier studies widely reported its utility as a diagnostic marker for angiogenesis in numerous cancer types, including renal cancer (Saroufim et al., 2014). Many recent studies suggest that CD105 has a tumor-intrinsic role in oncogenesis. Several studies indicate that CD105 plays a tumor-suppressive role in esophageal squamous cell carcinoma and prostate cancer (Henry et al., 2011; Wong et al., 2008). However, the preponderance of evidence suggests that CD105 promotes metastasis and chemoresistance (Dales et al., 2003; Pal et al., 2014). The opposing functional activity of CD105 might be attributed to its different isoforms. To date, three isoforms of CD105

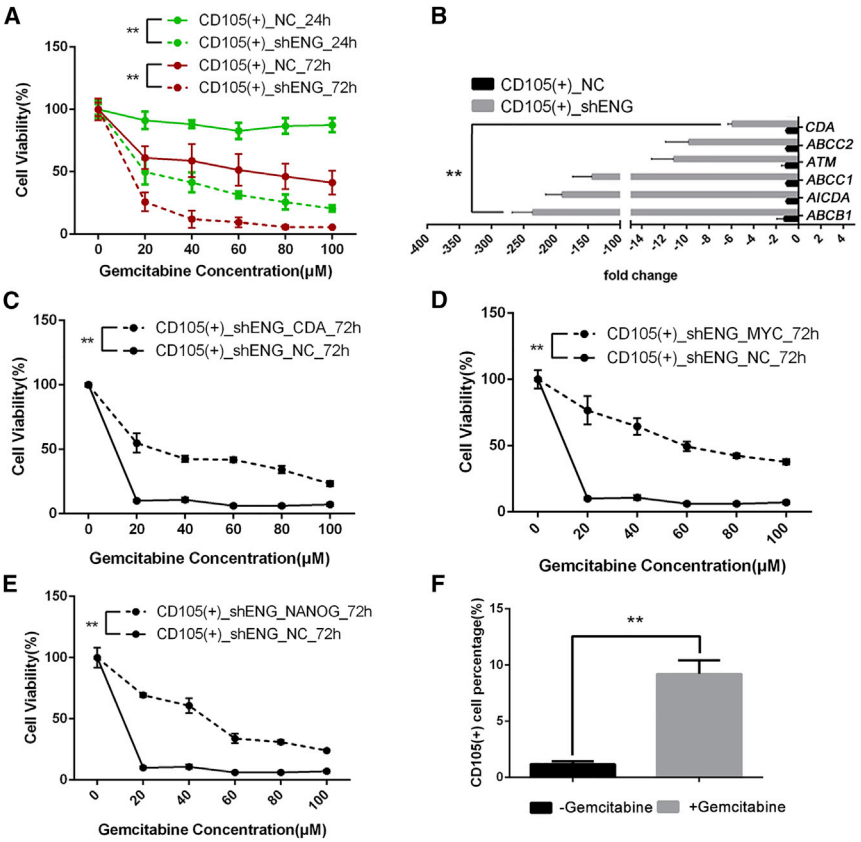

Figure 7. Knockdown of CD105 in CD105$^+$ Cells Abrogates Gemcitabine Resistance, and This Effect Can Be Reversed by Subsequent Overexpression of CDA, MYC, or NANOG

(A and B) Knockdown of CD105 in ACHN-CD105$^+$ resensitizes the cell line to gemcitabine (A) and reduces the expression of chemoresistance genes including CDA, ABCB1, and AICDA (B).

(C–E) Moreover, the overexpression of CDA (C), C-MYC (D), or NANOG (E) overcomes the resensitization to gemcitabine induced by CD105 knockdown. We also treated the subcutaneous xenograft model (ACHN cells) with gemcitabine or control via intraperitoneal injection in Balb/c-nu nude mice.

(F) The CD105 expression of the tumor samples was analyzed by flow cytometry, revealing a higher percentage of CD105$^+$ cells in the gemcitabine-treated tumors compared with control.

Three independent experiments were undertaken for each assay. **p < 0.01.

have been identified, namely CD105-L, CD105-S, and CD105-v3, with distinct extracellular and intracellular domains (Van Le et al., 2009; Velasco et al., 2008). CD105-v3 was discovered recently in 2015 and its role still remains unclear. Interestingly, CD105-L and CD105-S appear to mediate opposing effects on tumor cells. Velasco et al. (2008) reported that CD105-L promotes cell proliferation via ALK1/Smad1/Id1, and CD105-S inhibits cells' growth potential via the ALK5/Smad2/PAI1 pathway. Also, CD105-L has been shown to be proangiogenic, while CD105-S exerts the opposite effect (Perez-Gomez et al., 2005). Our preliminary analysis showed that the predominant form of CD105 in the sorted CD105$^+$ cells is CD105-L (data not shown). We are actively investigating the possible role of different CD105 isoforms in mediating CSC functions in RCC models.

Our findings suggest that overexpressing CDA, C-MYC, or NANOG independently can overcome the loss of CSC functions that resulted from the knockdown or knockout of CD105 (Figure S5). Importantly, as we overexpressed CD105-L in the parental cell line from ACHN xenograft, the gemcitabine resistance and sphere formation ability were both elevated (Figures S4B–S4D). In contrast to the increased apoptosis upon shRNA-mediated knockdown, the extent of cell senescence was also ameliorated upon CD105-L overexpression (Figure S4E). In line with our finding in kidney cancer cell xenografts, shRNA-mediated knockdown of CD105 can also decrease the self-renewal capability of CD105$^+$ cells sorted from ccRCC patient primary tumors (Figure S6). Coincidentally, CD105 therapeutic antibody has been on clinical trial in metastatic castration-resistant prostate cancer (mCRPC) (Karzai et al., 2015) and other tumors (Rosen et al., 2012). According to the phase I mCRPC trial, TRC105 was found to have a potential effect on the decrease of prostate-specific antigen velocity, which indicates a potential therapeutic role in mCRPC patients. Also, the clinical trial of TRC105 in combination with the multi-targeted receptor kinase inhibitor pazopanib on angiosarcoma has entered phase III (Clinical Trials, #NCT02979899). Even though the anti-CD105 agent TRC105 was developed as an anti-angiogenic drug, it is promising that it can also serve as an agent targeting the tumor-initiating cells in ccRCC.

CDA is a member of the cytidine deaminase protein family, which includes AID and APOBEC among others. For a long time CDA was presumed to only play a role in pyrimidine salvaging rather than in other fields, as its siblings do. In contrast, AID and APOBEC are actively involved in

class-switch recombination, immunoglobulin somatic hypermutation, and DNA demethylation (Muramatsu et al., 2000; Nabel et al., 2012). An abundance of evidence shows that AID/APOBEC can convert 5-mC (5-methylcytosine) to thymidine, which would be removed by T-G mismatch-specific glycosylase (Fritz and Papavasiliou, 2010; Ramiro and Barreto, 2016). The depleted sites can be subsequently replaced by an unmethylated cytidine in a base excision repair process, thereby demethylating the cytosine in the CpG island. In our study, we speculated that CDA also possesses a demethylation activity in a similar manner to AICDA/APOBEC in $CD105^+$ kidney cancer cells. Interestingly, as we knocked out CDA in $CD105^+$-ENG(KO)-CDA cells, the sphere-formation ability was diminished and accompanied by downregulation of NANOG and C-MYC (Figures S7A and S7B). However, as we applied 5-aza-2′-deoxycytidine in CDA knockout cell lines, the repressed NANOG and C-MYC protein were both elevated(Figure S7C), supporting that CDA might also serve as an important demethylase in $CD105^+$ cells. Nevertheless, further CpG island methylation status analysis on NANOG and MYC promoters is required to rule out other possible mechanisms and to validate our finding. Accordingly, a schematic illustration depicting the possible regulatory circuit is shown in Figure S7D.

With the ligand binding to TGFβ receptor, the activation of coreceptor endoglin-L can phosphorylate SMADs, which subsequently serve as transcriptional factors promoting the transcription of downstream proteins including CDA, NANOG, and C-MYC. C-MYC (Sussman et al., 2007; Varlakhanova et al., 2010) and NANOG (Chiou et al., 2010; Lee et al., 2011; Loh et al., 2006) are well-known critical transcription factors in both normal and malignant stem cells, and drive chemoresistance (Leonetti et al., 1999) by promoting either cell apoptosis or DNA repair (Figure S3E). In terms of the gemcitabine resistance, it is well established that overexpressed CDA can actively transform gemcitabine into its non-active form, thereby indirectly inhibiting the production of its active form 2′-difluorodeoxycytidine 5′-triphosphate. Also, we provide evidence hinting that CDA might also play a role as a demethylase over NANOG and C-MYC promoters and increase the transcription of these two genes (Mahfouz et al., 2013; Zauri et al., 2015). Thus, CDA could potentially play a role in activating critical stemness regulators such as NANOG and C-MYC.

Taken together, our study showed that CD105 can serve as a marker to isolate CSCs from human kidney cancer xenografts. Furthermore, CD105 plays a functional role in maintaining the stem cell phenotype of CSCs. NANOG, C-MYC, and CDA are three possible downstream mediators of CD105 that promote self-renewal and chemoresistance. Also, CDA might not only play a role as "shredder" of gemcitabine resulting in its resistance, but also may serve as a demethylase enhancing other genes' transcription. As such, CD105 could be a promising therapeutic target to overcome resistant or recurrent kidney cancer.

EXPERIMENTAL PROCEDURES

Plasmids, Antibodies, and Reagents

The shRNA plasmids for CD105 knockdown were constructed from pSicoR (Addgene, #11579) with target sequences of shENG1: GAA AGA GCT TGT TGC GCA T and shENG2: AAC AGT CCA TTG TGA CCT TCA. Data presented were from knockdown with shEGN1, which is consistent with the results from shENG2 (Figure S3). The ectopic overexpression plasmids of ENG, CDA, MYC, and NANOG were constructed based on the basic lentiviral vector.

Regarding antibodies, anti-human OCT-4 (#ab19857), SOX-2 (#ab171380), KLF4 (#ab72543), NANOG (#ab80892), and C-MYC (#ab32072) were bought from Abcam (MA, USA), anti-human ACTIN (#AC026) was bought from Abclonal (MA, USA), anti-human CD105 (#ab169545), CD44 (#ab51037), MUSASHI (#EP1302), NESTIN (#ab105389), and VIMENTIN (#ab16700) were bought from Epitomics (CA, USA), anti-human MHC-I (#GTX105052) and CK7(#GTX109723) were bought from Genetex (CA, USA), and anti-human DLK-1(#AP20959c) and CXCR4 (#AW5434-U080) were bought from Abgent (CA, USA). For flow cytometry, anti-human CD105 conjugated with PE antibody (#130-098-906) was bought from Miltenyi (CA, USA).

Ethics Statement

All the protocols in this study were approved by the Ethics Committee of Tongji Hospital affiliated with Tongji Medical School, Huazhong University of Science and Technology (HUST). Written consent was obtained from patients whose tissues were collected for analysis in this study. All mice in our experiments were kept in the Specific Pathogen Free (SPF) animal center in Tongji Medical School, and this study was designed to abide by the principles stated in the Declaration of Helsinki.

$CD105^+$ Kidney Cancer Cell Subpopulation Isolation and Maintenance

The kidney cancer cell line ACHN was purchased from ATCC (Manassas, VA, USA) and maintained at 37°C in 5% CO_2 in DMEM-HG (Hyclone, USA) with 10% FBS (Hyclone). A total of 1.0×10^6 ACHN cells were transplanted subcutaneously in the right axillary fossa of male Balb/c-nu mice. After 1 month of growth, the tumor was minced with a sterile scalpel and digested with 0.2% collagenase II (Solarbio, Beijing, China) at 37°C for 2 hr with shaking. After washes in PBS, tumor cells were stained with anti-human CD105-PE antibody (Miltenyi Biotec, CA, USA, #130-098-906) for 1 hr at 4°C and sorted using an MoFlo XDP cell sorter (Beckman Coulter, USA). The parental cell line and the sorted $CD105^+$ cancer cell subpopulation were maintained in the renal CSC expansion medium as described by Bussolati et al. (2008). The isolation process is summarized in Figure S1A. Expression of CD105 and the stemness markers as *OCT-4*, *NANOG*,

SOX-2, *Klf-4*, and C-*MYC* were examined every month to confirm their stemness within 50 passages.

786-O, HK-2, OS-RC-2, CAKI-1, and U937 were purchased from Shanghai Institute for Biological Sciences of the Chinese Academy of Sciences. SN12-PM6 cells were a kind gift from Xiaoping Zhang at Union Hospital affiliated to Huazhong University of Science and Technology in Wuhan, China.

In Vivo Orthotopic Xenograft Assay with Limiting Diluted Cells and *In Vivo* Imaging

In vivo tumorigenicity of cancer cells was determined using limiting dilution xenografts. $CD105^+$ labeled with EGFP and control shRNA targeting firefly luciferase, parental cell line labeled with EGFP and control shRNA, and $CD105^+$_shENG-EGFP cells labeled with EGFP and shRNA targeting CD105 were cultured in expansion medium. NOD/SCID mice were injected with serial dilutions of cells: 1.0×10^2, 1.0×10^4, and 1.0×10^6, respectively, with five male NOD/SCID mice per dilution. Cells were trypsinized, rinsed with PBS, and resuspended in 20 μL of Matrigel diluted with precooled PBS at the ratio of 1:1. Four-week-old mice were then anesthetized with sterilized 1% pentobarbital sodium at the dose of 10 mL/kg via intraperitoneal injection. The back of each mouse was shaved and the right kidney injected with 20 μL of cells. After 2 months, 45 mice (15 mice for each cell line, 5 per dilution for each cell type) were euthanized with cervical dislocation and sent for *in vivo* fluorescence imaging with a home-made whole-body fluorescence imaging system (Luo et al., 2014; Qian et al., 2016; Yang et al., 2012). The fluorescence signal of EGFP was detected through a filter set (excitation 469/35 nm, emission: 510/42 nm). Kidneys from three mice (two kidneys for each mouse, one with tumor and the other serving as control) in each cell dilution of each group are shown in Figures 4 and 6.

In Vivo Gemcitabine-Resistant Assay of $CD105^+$ Cells in Subcutaneous Xenograft Model

An *in vivo* subcutaneous xenograft model with ACHN cells was established to assess the gemcitabine resistance of $CD105^+$ cells. Ten male 4-week-old Balb/c-nu mice were randomly grouped into two groups (5 mice per group). A total of 1×10^6 ACHN cells were resuspended in 100 μL of diluted Matrigel (Matrigel and precooled PBS in a volume ratio of 1:2) and then injected subcutaneously into the right axillary fossa of each mouse. When the tumor reached 0.5 cm in diameter, one group of mice was administered gemcitabine, 0.015 mg/g/day, via intraperitoneal injection on the first, third, sixth, and ninth day while control mice received intraperitoneal injection with saline. Ten days after initial treatment, both groups of mice were euthanized and tumors were resected for flow-cytometric analysis. CD105 expression was described as above.

Statistical Analysis

Each experiment was performed at least in triplicate unless otherwise stated. Data are presented as mean ± SD. Significance was determined by a paired, Student's t test when there were two groups or by one-way ANOVA when there were three or more groups (GraphPad Prism ver6.0). A p value cutoff of 0.05 was used to establish significance. Additional methods and materials are described in Supplemental Experimental Procedures.

SUPPLEMENTAL INFORMATION

Supplemental Information includes Supplemental Experimental Procedures, seven figures, and one table and can be found with this article online at http://dx.doi.org/10.1016/j.stemcr.2017.07.009.

AUTHOR CONTRIBUTIONS

J.H. and W.G. wrote, reviewed, and revised the manuscript and designed the experiments; L.W. and H. Xu reviewed and revised the manuscript, designed the experiments, and supervised the study; J.H., W.G., P.L., J.D., K.T., and H. Xiao developed the methodology and analyzed and interpreted the data; Y.Q. performed the *in vivo* imaging experiment and analyzed and interpreted the data; A.C.S. helped in proofreading and revision of the manuscript; Z.Y., L.W., and H. Xu provided the administrative, technical, and material support.

ACKNOWLEDGMENTS

This work was supported by the National Natural Science Foundation of China (31372562, 81470935), the National Major Scientific and Technological Special Project for Significant New Drugs Development (2012ZX09303018), the Chenguang Program of Wuhan Science and Technology Bureau (2015070404010199), and the National High Technology Research and Development Program 863 (2014AA020607). The funders had no role in study design, data collection and analysis, decision to publish, or preparation of the manuscript. We thank all the donors who participated in this program and all our coworkers who contributed to the construction of the urologic tumor tissue bank sponsored by the Department of Urology, Tongji Hospital, Tongji Medical College, Huazhong University of Science and Technology. Also, the technical support in *in vivo* imaging from Dr. Qingming Luo and Dr. Zhihong Zhang from the Britton Chance Center for Biomedical Photonics in HUST and support in cell sorting from Mr. Peng Xu in YZY Bioscience Corp. in Wuhan are greatly appreciated.

Received: December 6, 2016
Revised: July 10, 2017
Accepted: July 11, 2017
Published: August 8, 2017

REFERENCES

Abdullah, L.N., and Chow, E.K.-H. (2013). Mechanisms of chemoresistance in cancer stem cells. Clin. Transl. Med. *2*, 3.

Azzi, S., Bruno, S., Giron-Michel, J., Clay, D., Devocelle, A., Croce, M., Ferrini, S., Chouaib, S., Vazquez, A., Charpentier, B., et al. (2011). Differentiation therapy: targeting human renal cancer stem cells with interleukin 15. J. Natl. Cancer Inst. *103*, 1884–1898.

Beier, D., Hau, P., Proescholdt, M., Lohmeier, A., Wischhusen, J., Oefner, P.J., Aigner, L., Brawanski, A., Bogdahn, U., and Beier, C.P. (2007). $CD133^+$ and $CD133^-$ glioblastoma-derived cancer

stem cells show differential growth characteristics and molecular profiles. Cancer Res. *67*, 4010–4015.

Beier, D., Schulz, J.B., and Beier, C.P. (2011). Chemoresistance of glioblastoma cancer stem cells—much more complex than expected. Mol. Cancer *10*, 128.

Borovski, T., De Sousa, E.M.F., Vermeulen, L., and Medema, J.P. (2011). Cancer stem cell niche: the place to be. Cancer Res. *71*, 634–639.

Bussolati, B., Bruno, S., Grange, C., Ferrando, U., and Camussi, G. (2008). Identification of a tumor-initiating stem cell population in human renal carcinomas. FASEB J. *22*, 3696–3705.

Canino, C., Luo, Y., Marcato, P., Blandino, G., Pass, H.I., and Cioce, M. (2015). A STAT3-NFkB/DDIT3/CEBPβ axis modulates ALDH1A3 expression in chemoresistant cell subpopulations. Oncotarget *6*, 12637–12653.

Chen, X., Sun, K., Jiao, S., Cai, N., Zhao, X., Zou, H., Xie, Y., Wang, Z., Zhong, M., and Wei, L. (2014). High levels of SIRT1 expression enhance tumorigenesis and associate with a poor prognosis of colorectal carcinoma patients. Sci. Rep. *4*, 7481.

Chiou, S.-H., Wang, M.-L., Chou, Y.-T., Chen, C.-J., Hong, C.-F., Hsieh, W.-J., Chang, H.-T., Chen, Y.-S., Lin, T.-W., Hsu, H.-S., et al. (2010). Coexpression of Oct4 and NANOG enhances malignancy in lung adenocarcinoma by inducing cancer stem cell–like properties and epithelial-mesenchymal transdifferentiation. Cancer Res. *70*, 10433–10444.

Dales, J.P., Garcia, S., Bonnier, P., Duffaud, F., Andrac-Meyer, L., Ramuz, O., Lavaut, M.N., Allasia, C., and Charpin, C. (2003). CD105 expression is a marker of high metastatic risk and poor outcome in breast carcinomas. Correlations between immunohistochemical analysis and long-term follow-up in a series of 929 patients. Am. J. Clin. Pathol. *119*, 374–380.

Escudier, B., Cosaert, J., and Jethwa, S. (2008). Targeted therapies in the management of renal cell carcinoma: role of bevacizumab. Biologics *2*, 517–530.

Fritz, E.L., and Papavasiliou, F.N. (2010). Cytidine deaminases: AIDing DNA demethylation? Genes Dev. *24*, 2107–2114.

Guerrero-Esteo, M., Sanchez-Elsner, T., Letamendia, A., and Bernabeu, C. (2002). Extracellular and cytoplasmic domains of Endoglin interact with the transforming growth factor-beta receptors I and II. J. Biol. Chem. *277*, 29197–29209.

Henry, L.A., Johnson, D.A., Sarrio, D., Lee, S., Quinlan, P.R., Crook, T., Thompson, A.M., Reis-Filho, J.S., and Isacke, C.M. (2011). Endoglin expression in breast tumor cells suppresses invasion and metastasis and correlates with improved clinical outcome. Oncogene *30*, 1046–1058.

Hoffman, A.M., and Cairns, P. (2011). Epigenetics of kidney cancer and bladder cancer. Epigenomics *3*, 19–34.

Huang, B., Huang, Y.J., Yao, Z.J., Chen, X., Guo, S.J., Mao, X.P., Wang, D.H., Chen, J.X., and Qiu, S.P. (2013). Cancer stem cell-like side population cells in clear cell renal cell carcinoma cell line 769P. PLoS One *8*, e68293.

Kamohara, Y., Haraguchi, N., Mimori, K., Tanaka, F., Inoue, H., Mori, M., and Kanematsu, T. (2008). The search for cancer stem cells in hepatocellular carcinoma. Surgery *144*, 119–124.

Kandyba, E., Hazen, V.M., Kobielak, A., Butler, S.J., and Kobielak, K. (2014). Smad1 and 5 but not Smad8 establish stem cell quiescence which is critical to transform the premature hair follicle during morphogenesis toward the postnatal state. Stem Cells *32*, 534–547.

Karzai, F.H., Apolo, A.B., Cao, L., Madan, R.A., Adelberg, D.E., Parnes, H., McLeod, D.G., Harold, N., Peer, C., Yu, Y., et al. (2015). A phase I study of TRC105 anti-Endoglin (CD105) antibody in metastatic castration-resistant prostate cancer. BJU Int. *116*, 546–555.

Khan, M.I., Czarnecka, A.M., Lewicki, S., Helbrecht, I., Brodaczewska, K., Koch, I., Zdanowski, R., Król, M., and Szczylik, C. (2016). Comparative gene expression profiling of primary and metastatic renal cell carcinoma stem cell-like cancer cells. PLoS One *11*, e0165718.

Kim, S.H., Joshi, K., Ezhilarasan, R., Myers, T.R., Siu, J., Gu, C., Nakano-Okuno, M., Taylor, D., Minata, M., Sulman, E.P., et al. (2015). EZH2 protects glioma stem cells from radiation-induced cell death in a MELK/FOXM1-dependent manner. Stem Cell Rep. *4*, 226–238.

Koleva, R.I., Conley, B.A., Romero, D., Riley, K.S., Marto, J.A., Lux, A., and Vary, C.P. (2006). Endoglin structure and function: determinants of Endoglin phosphorylation by transforming growth factor-beta receptors. J. Biol. Chem. *281*, 25110–25123.

Kumar, S.M., Liu, S., Lu, H., Zhang, H., Zhang, P.J., Gimotty, P.A., Guerra, M., Guo, W., and Xu, X. (2012). Acquired cancer stem cell phenotypes through Oct4-mediated dedifferentiation. Oncogene *31*, 4898–4911.

Larkin, J.M.G., and Eisen, T. (2006). Renal cell carcinoma and the use of sorafenib. Ther. Clin. Risk Manag. *2*, 87–98.

Lee, T.K., Castilho, A., Cheung, V.C., Tang, K.H., Ma, S., and Ng, I.O. (2011). CD24(+) liver tumor-initiating cells drive self-renewal and tumor initiation through STAT3-mediated NANOG regulation. Cell Stem Cell *9*, 50–63.

Leonetti, C., Biroccio, A., Candiloro, A., Citro, G., Fornari, C., Mottolese, M., Bufalo, D.D., and Zupi, G. (1999). Increase of cisplatin sensitivity by c-myc antisense oligodeoxynucleotides in a human metastatic melanoma inherently resistant to cisplatin. Clin. Cancer Res. *5*, 2588–2595.

Li, L., Candelario, K.M., Thomas, K., Wang, R., and Wright, K. (2014). Hypoxia inducible factor-1alpha (HIF-1alpha) is required for neural stem cell maintenance and vascular stability in the adult mouse SVZ. J. Neurosci. *34*, 16713–16719.

Linehan, W.M., and Rathmell, W.K. (2012). Kidney cancer. Urol. Oncol. *30*, 948–951.

Loh, Y.H., Wu, Q., Chew, J.L., Vega, V.B., Zhang, W., Chen, X., Bourque, G., George, J., Leong, B., Liu, J., et al. (2006). The Oct4 and NANOG transcription network regulates pluripotency in mouse embryonic stem cells. Nat. Genet. *38*, 431–440.

Luo, H., Lu, L., Yang, F., Wang, L., Yang, X., Luo, Q., and Zhang, Z. (2014). Nasopharyngeal cancer-specific therapy based on fusion peptide-functionalized lipid nanoparticles. ACS Nano *8*, 4334–4347.

Ma, S., Lee, T.K., Zheng, B.J., Chan, K.W., and Guan, X.Y. (2008). CD133+ HCC cancer stem cells confer chemoresistance by preferential expression of the Akt/PKB survival pathway. Oncogene *27*, 1749–1758.

Mahfouz, R.Z., Jankowska, A., Ebrahem, Q., Gu, X., Visconte, V., Tabarroki, A., Terse, P., Covey, J., Chan, K., Ling, Y., et al. (2013). Increased CDA expression/activity in males contributes to decreased cytidine analog half-life and likely contributes to worse outcomes with 5-azacytidine or decitabine therapy. Clin. Cancer Res. *19*, 938–948.

Maugeri-Saccà, M., Bartucci, M., and De Maria, R. (2012). DNA damage repair pathways in cancer stem cells. Mol. Cancer Ther. *11*, 1627–1636.

Muramatsu, M., Kinoshita, K., Fagarasan, S., Yamada, S., Shinkai, Y., and Honjo, T. (2000). Class switch recombination and hypermutation require activation-induced cytidine deaminase (AID), a potential RNA editing enzyme. Cell *102*, 553–563.

Nabel, C.S., Jia, H., Ye, Y., Shen, L., Goldschmidt, H.L., Stivers, J.T., Zhang, Y., and Kohli, R.M. (2012). AID/APOBEC deaminases disfavor modified cytosines implicated in DNA demethylation. Nat. Chem. Biol. *8*, 751–758.

Naito, S., Walker, S.M., and Fidler, I.J. (1989). In vivo selection of human renal cell carcinoma cells with high metastatic potential in nude mice. Clin. Exp. Metastasis *7*, 381–389.

Pal, K., Pletnev, A.A., Dutta, S.K., Wang, E., Zhao, R., Baral, A., Yadav, V.K., Aggarwal, S., Krishnaswamy, S., Alkharfy, K.M., et al. (2014). Inhibition of Endoglin-GIPC interaction inhibits pancreatic cancer cell growth. Mol. Cancer Ther. *13*, 2264–2275.

Paldino, E., Tesori, V., Casalbore, P., Gasbarrini, A., and Puglisi, M.A. (2014). Tumor initiating cells and chemoresistance: which is the best strategy to target colon cancer stem cells? Biomed. Res. Int. *2014*, 859871.

Pantuck, A.J., An, J., Liu, H., and Rettig, M.B. (2010). NF-κB-dependent plasticity of the epithelial to mesenchymal transition induced by von hippel-lindau inactivation in renal cell carcinomas. Cancer Res. *70*, 752–761.

Parodi, B., Aresu, O., Bini, D., Lorenzini, R., Schena, F., Visconti, P., Cesaro, M., Ferrera, D., Andreotti, V., and Ruzzon, T. (2002). Species identification and confirmation of human and animal cell lines: a PCR-based method. Biotechniques *32*, 432–434, 436, 438–440.

Perez-Gomez, E., Eleno, N., Lopez-Novoa, J.M., Ramirez, J.R., Velasco, B., Letarte, M., Bernabeu, C., and Quintanilla, M. (2005). Characterization of murine S-Endoglin isoform and its effects on tumor development. Oncogene *24*, 4450–4461.

Qian, Y., Jin, H., Qiao, S., Dai, Y., Huang, C., Lu, L., Luo, Q., and Zhang, Z. (2016). Targeting dendritic cells in lymph node with an antigen peptide-based nanovaccine for cancer immunotherapy. Biomaterials *98*, 171–183.

Ramiro, A.R., and Barreto, V.M. (2016). Activation-induced cytidine deaminase and active cytidine demethylation. Trends Biochem. Sci. *40*, 172–181.

Rini, B.I., Campbell, S.C., and Escudier, B. (2009). Renal cell carcinoma. Lancet *373*, 1119–1132.

Roesch, A., Fukunaga-Kalabis, M., Schmidt, E.C., Zabierowski, S.E., Brafford, P.A., Vultur, A., Basu, D., Gimotty, P., Vogt, T., and Herlyn, M. (2010). A temporarily distinct subpopulation of slow-cycling melanoma cells is required for continuous tumor growth. Cell *141*, 583–594.

Rosen, L.S., Hurwitz, H.I., Wong, M.K., Goldman, J., Mendelson, D.S., Figg, W.D., Spencer, S., Adams, B.J., Alvarez, D., Seon, B.K., et al. (2012). A phase I first-in-human study of TRC105 (Anti-Endoglin Antibody) in patients with advanced cancer. Clin. Cancer Res. *18*, 4820–4829.

Sakaki-Yumoto, M., Liu, J., Ramalho-Santos, M., Yoshida, N., and Derynck, R. (2013). Smad2 is essential for maintenance of the human and mouse primed pluripotent stem cell state. J. Biol. Chem. *288*, 18546–18560.

Saroufim, A., Messai, Y., Hasmim, M., Rioux, N., Iacovelli, R., Verhoest, G., Bensalah, K., Patard, J.J., Albiges, L., Azzarone, B., et al. (2014). Tumoral CD105 is a novel independent prognostic marker for prognosis in clear-cell renal cell carcinoma. Br. J. Cancer *110*, 1778–1784.

Schokrpur, S., Hu, J., Moughon, D.L., Liu, P., Lin, L.C., Hermann, K., Mangul, S., Guan, W., Pellegrini, M., Xu, H., et al. (2016). CRISPR-mediated VHL knockout generates an improved model for metastatic renal cell carcinoma. Sci. Rep. *6*, 29032.

Shen, C., Beroukhim, R., Schumacher, S.E., Zhou, J., Chang, M., Signoretti, S., and Kaelin, W.G. (2011). Genetic and functional studies implicate HIF1α as a 14q kidney cancer suppressor gene. Cancer Discov. *1*, 222–235.

Siegel, R., Naishadham, D., and Jemal, A. (2013). Cancer statistics, 2013. CA Cancer J. Clin. *63*, 11–30.

Sudarshan, S., Karam, J.A., Brugarolas, J., Thompson, R.H., Uzzo, R., Rini, B., Margulis, V., Patard, J.J., Escudier, B., and Linehan, W.M. (2013). Metabolism of kidney cancer: from the lab to clinical practice. Eur. Urol. *63*, 244–251.

Sussman, R.T., Ricci, M.S., Hart, L.S., Sun, S.Y., and El-Deiry, W.S. (2007). Chemotherapy-resistant side-population of colon cancer cells has a higher sensitivity to TRAIL than the non-SP, a higher expression of c-Myc and TRAIL-receptor DR4. Cancer Biol. Ther. *6*, 1490–1495.

Van Le, B., Franke, D., Svergun, D.I., Han, T., Hwang, H.Y., and Kim, K.K. (2009). Structural and functional characterization of soluble Endoglin receptor. Biochem. Biophys. Res. Commun. *383*, 386–391.

Varlakhanova, N.V., Cotterman, R.F., deVries, W.N., Morgan, J., Donahue, L.R., Murray, S., Knowles, B.B., and Knoepfler, P.S. (2010). Myc maintains embryonic stem cell pluripotency and self-renewal. Differentiation *80*, 9–19.

Velasco, S., Alvarez-Munoz, P., Pericacho, M., Dijke, P.T., Bernabeu, C., Lopez-Novoa, J.M., and Rodriguez-Barbero, A. (2008). L- and S-Endoglin differentially modulate TGFbeta1 signaling mediated by ALK1 and ALK5 in L6E9 myoblasts. J. Cell Sci. *121*, 913–919.

Whalley, K. (2011). Stem cells: a niche role for DLK1. Nat. Rev. Neurosci. *12*, 489.

Wong, V.C., Chan, P.L., Bernabeu, C., Law, S., Wang, L.D., Li, J.L., Tsao, S.W., Srivastava, G., and Lung, M.L. (2008). Identification of an invasion and tumor-suppressing gene, Endoglin (ENG), silenced by both epigenetic inactivation and allelic loss in esophageal squamous cell carcinoma. Int. J. Cancer *123*, 2816–2823.

Yang, X., Gong, H., Fu, J., Quan, G., Huang, C., and Luo, Q. (2012). Molecular imaging of small animals with fluorescent proteins: from projection to multimodality. Comput. Med. Imaging Graph. *36*, 259–263.

Zauri, M., Berridge, G., Thezenas, M.-L., Pugh, K.M., Goldin, R., Kessler, B.M., and Kriaucionis, S. (2015). CDA directs metabolism of epigenetic nucleosides revealing a therapeutic window in cancer. Nature *524*, 114–118.

Zhong, Y., Guan, K., Guo, S., Zhou, C., Wang, D., Ma, W., Zhang, Y., Li, C., and Zhang, S. (2010). Spheres derived from the human SK-RC-42 renal cell carcinoma cell line are enriched in cancer stem cells. Cancer Lett. *299*, 150–160.